European Polymer Journal 130 (2020) 109624

Contents lists available at ScienceDirect

European Polymer Journal

journal homepage: www.elsevier.com/locate/europolj

Fast dissolving nanofibrous matrices prepared by electrospinning of polyaspartamides

Csaba Németh[a], Benjámin Gyarmati[a], Jenő Gacs[a], Diana V. Salakhieva[d], Kolos Molnár[b,c], Timur Abdullin[d], Krisztina László[a], András Szilágyi[a,*]

[a] Department of Physical Chemistry and Materials Science, Budapest University of Technology and Economics, Műegyetem rkp. 3., H-1111 Budapest, Hungary
[b] Department of Polymer Engineering, Budapest University of Technology and Economics, Műegyetem rkp. 3., H-1111 Budapest, Hungary
[c] MTA–BME Research Group for Composite Science and Technology, Műegyetem rkp. 3., H-1111 Budapest, Hungary
[d] Institute of Fundamental Medicine and Biology, Kazan (Volga Region) Federal University, 18 Kremlyovskaya str., 420008 Kazan, Russia

ARTICLE INFO

Keywords:
Electrospinning
Cationic polyaspartamides
Nanofibrous matrix
Sublingual drug delivery

ABSTRACT

Owing to their versatile chemistry, polyaspartamides have recently attracted increased interest in various biomedical uses such as drug delivery systems and scaffolding materials. Solubility of these polymers in organic solvents and in water at certain values of pH can be fine-tuned by their chemical composition, which was exploited here to fabricate fast-dissolving electrospun matrices in ethanol with no additives. Various side groups were tested to control the solubility of the polymers as well as the morphology and moisture uptake of the matrices produced. Tertiary amine groups were immobilized to ensure high solubility around neutral pH, while modification with alkyl side groups limited moisture uptake. Finally, 3-(diethylamino)propyl and *n*-butyl side groups were used in equal amounts. The effect of viscosity, surface tension and specific conductivity of polymer solutions on the fiber morphology was determined in order to optimize the conditions for preparing fibers with a narrow size distribution and large specific surface area. The polymer withstood the electrospinning process without any chemical degradation, as determined by IR, and was thermally stable. Furthermore, the matrices exhibited a glass transition temperature above room temperature. The complete release of vitamin B_{12} was observed within one minute due to the fast dissolution of the matrices in simulated salivary fluid at pH = 6.8, supporting the potential of the developed materials in oral drug delivery.

1. Introduction

Oral transmucosal (sublingual and buccal) drug delivery can substantially increase the bioavailability of drugs by their rapid absorption through the mucous membranes of the oral cavity. The drugs absorbed by this route are not exposed to degradation in the gastrointestinal tract and the hepatic first-pass metabolism is bypassed [1,2]. Commercially available formulations do not exploit the full potential of the oral transmucosal route, which has directed considerable attention towards electrospun polymer matrices with micro or nanofibrous morphology [3–5]. The large specific surface area of electrospun matrices provides fast dissolution and rapid drug release, while the rate can be controlled by the morphology of the fibers. The shape and diameter of the fibers can be tailored both through the properties of the pre-cursor material (polymer composition, concentration, dielectric constant of the solvent, etc.) and the technological parameters of the electrospinning (applied voltage, flow rate, etc.) [6–8]. Drug molecules can be loaded into the matrices in their amorphous state, which further helps their rapid dissolution in aqueous medium [9,10]. Finally, contrary to sprays, suspensions or drops; the drugs can easily be administered in an exact dose from electrospun matrices.

Electrospun materials are mainly prepared from synthetic polymers such as poly(meth)acrylates, poly(vinyl alcohol), poly(vinyl acetate) and polyvinylpyrrolidone, but also from natural and natural based polymers such as cellulose derivatives and poly(lactic acid). Electrospinning of these polymers commonly requires the use of toxic or corrosive solvents, which should be avoided in pharmaceutical applications. Dimethylformamide, chloroform and dichloromethane are commonly used [11,12], despite the fact that their residual quantities are strictly limited in pharmaceutical products (ICH Class 2 solvents, concentration limit ~10 ppm [13,14]). The problem can be overcome potentially by the use of aqueous medium or melt electrospinning [15], but these methods cannot be applied for hydrolytically or thermally unstable drugs as well as molecules with low aqueous solubility [16].

* Corresponding author.
E-mail address: aszilagyi@mail.bme.hu (A. Szilágyi).

https://doi.org/10.1016/j.eurpolymj.2020.109624
Received 14 November 2019; Received in revised form 13 March 2020; Accepted 16 March 2020
Available online 17 March 2020

Ethanol, a green solvent (ICH Class 3, concentration limit: ~5000 ppm [13,17]), can extend the application of electrospinning for pharmaceutical purposes, however the range of available ethanol soluble polymers is quite limited. The proper derivatization of poly(meth)acrylates [18,19], polyvinylpyrrolidone [20,21], poly(ethylene oxide) [9,22], poly(vinyl acetate) [23] or hydroxypropyl cellulose [24] involves complex synthetic pathways and most of these polymers lack biodegradability. Consequently, the use of a biocompatible, biodegradable polymer with facile functionalization can open new possibilities in electrospinning from ethanol.

In recent years, polypeptides have attracted particular attention in electrospinning technology, especially in electrospun matrices for biomedical applications [25]. Natural polypeptides, such as gelatin, collagen and silk have the benefits of preparation from renewable sources and excellent cellular compatibility [26,27]. However, the structure of these polymers is variable and their chemical modification is difficult. Moreover, toxic and hazardous solvents (fluorinated alcohols and acids, dichloromethane) [28] and additional polymers (PEO, PCL) are required to obtain uniform and bead-free fibers from polypeptides [29]. Drawbacks of natural polypeptides can be overcome by employing synthetic poly(amino acid)s and analogues of polypeptides. Polysuccinimide [30–32], poly(γ-glutamic acid) [33] and poly(2-oxazoline) [34] have already been used, but apart from them, poly(aspartic acid) (PASP) derivatives also provide the chemical versatility needed for electrospinning in various solvents. The precursor polymer of PASP, polysuccinimide (PSI) reacts with primary amines under mild reaction conditions [35–39], which is of great interest for biomedical applications of PASP derivatives [40–42].

In our work, we prepared cationic polyaspartamides for electrospinning, as these polyaspartamides are highly soluble in water over a wide pH range, including that of the oral cavity (pH = 6.8), and are also soluble in pharmaceutically accepted alcohols (ICH Class 3, [13,17]), such as ethanol and 2-propanol [36]. These polymers were proven to be low-toxic on different cell lines [43] and, owing to their polypeptide structure, they are expected to be biodegradable [40]. Although there are some reports on the synthesis of cationic polyaspartamides [44,45], no attempt has been made to electrospin cationic polyaspartamides yet. The few reported fibrous matrices prepared from PASP derivatives were electrospun from toxic ICH Class 2 solvents, dimethylformamide or chloroform [30–32,46,47].

Our aim was to prepare cationic polyaspartamide matrices with rapid dissolution at the pH of the oral cavity. The polymer was synthesized by reacting polysuccinimide (PSI) with 3-(diethylamino)propylamine, and then with *n*-butylamine (DEP50B50). The chemical structure was confirmed by ^{1}H NMR and FTIR spectroscopy. The polymer was electrospun from ethanol. The viscosity, the surface tension and the specific conductivity of the polymer solutions were determined to select the proper conditions for electrospinning. The morphology of the nanofiber matrices was investigated by scanning electron microscopy (SEM). The glass transition temperature (T_g) of the matrices was determined by differential scanning calorimetry (DSC), and the thermal decomposition temperature (T_d) was characterized by thermogravimetric analysis (TGA). The dissolution kinetics of the polymer matrix and the drug release kinetics were determined to demonstrate a possible application of the matrix as a sublingual delivery system.

2. Experimental

2.1. Materials

2-(dimethylamino)ethylamine (DME, 98%), 2-(diethylamino)ethylamine (DEE, 99%), 3-(dimethylamino)propylamine (DMP, 98%), phosphoric acid (99%), *L*-tryptophan methyl ester hydrochloride (T), triethyl citrate (TEC, 98%), DMSO-d_6 and vitamin B_{12} were purchased from Sigma–Aldrich. *L*-aspartic acid (99%), 3-(diethylamino)propylamine (DEP, 98%), *n*-butylamine (B, 99%), dibutylamine (DBA, 99%), potassium chloride (99.5%), disodium hydrogen phosphate dihydrate (99.5%), potassium dihydrogen phosphate (99.5%) and dimethyl sulfoxide (DMSO, 99.9%) were obtained from Merck. Hydrochloric acid (HCl, 35%) and ethyl acetate (EtAc, 99.9%) were bought from LachNer. *N,N*-dimethylformamide (99.9%) and ethanol (99.7%) was purchased from Reanal. Saliva was simulated by a pH = 6.8 phosphate buffer [simulated salivary fluid (SSF), I = 0.15 M]. The pH of the buffer solution was checked with a pH/ion analyzer (Radelkis OP 271/1). All reagents were used without further purification unless otherwise noted. Ultrapure water (ρ > 18.2 MΩ cm, Millipore) was used for the preparation of aqueous solutions. Experiments were performed at room temperature (T = 25 °C) unless otherwise indicated.

2.2. Synthesis and preparation

2.2.1. Synthesis of the cationic polyaspartamides

Polysuccinimide (PSI) was synthesized by thermal polycondensation of *L*-aspartic acid in a solvent-free reaction using phosphoric acid as a catalyst [36]. The synthesis was carried out in a rotary evaporator, the temperature and pressure being maintained at 200 °C and 10 mbar during the reaction. A slightly brown product was formed after 5 h. PSI was purified by precipitation in DMF–H_2O (1:3) and dried in vacuum at 25 °C for 24 h. ^{1}H NMR (300 MHz, DMSO-d_6, δ) [ppm]: 5.27 (1H, CO–*CH*–CH_2–CO); 3.22 and 2.74 (2H, CO–CH–*CH_2*–CO). The viscosity average molecular weight was 29 kDa, determined by viscometry using an Anton Paar Lovis 2000 rolling ball viscometer [36].

In a typical procedure PSI was modified with 50 mol% 3-(diethylamino)propylamine (DEP) and subsequently with 50 mol% *n*-butylamine (B), resulting in a cationic polyaspartamide designated as DEP50B50. The synthesis was done in the following way (Scheme 1). 2.000 g of PSI (20.62 mmol succinimide unit) was dissolved in 18.0 g of DMSO and then 1.343 g (10.31 mmol) of DEP was added drop-wise to the solution. The mixture was stirred at room temperature for 24 h. 0.98 g of *n*-butylamine (13.40 mmol, in excess) was then added drop-wise to the solution and the mixture was stirred at room temperature

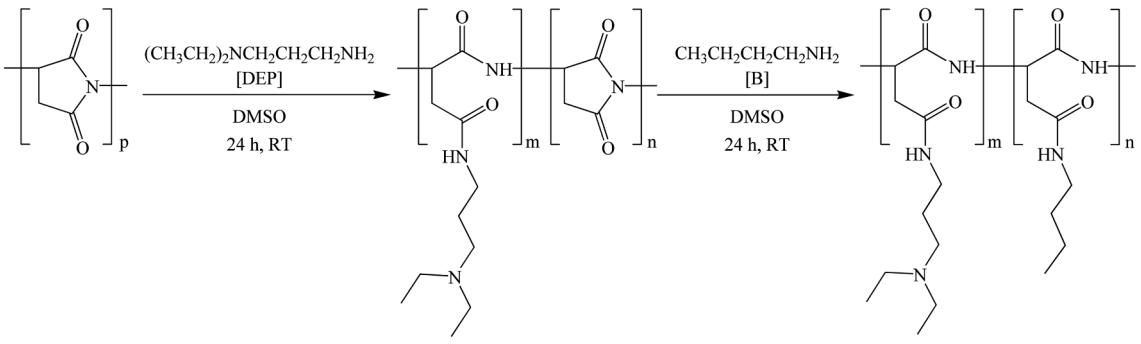

Scheme 1. Synthesis of DEP50B50 via reacting polysuccinimide (PSI) with 50 mol% 3-(diethylamino)propylamine (DEP) and 50 mol% *n*-butylamine (B).

for another 24 h. The polymer was precipitated by adding 300 ml of ethyl acetate to the reaction mixture, the precipitate was filtered and washed four times with 50 ml of ethyl acetate, then dried under vacuum at 25 °C for 24 h. A slightly yellow powder was obtained with an average yield of 75%. The polymer was stored at room temperature.

^{1}H NMR (500 MHz, DMSO-d_6, δ) [ppm]: 4.55 (1H, CO-*CH*-CH_2-CO), 3.06 (4H, NH-*CH_2*-CH_2-CH_2-N(CH_2CH_3)$_2$, NH-*CH_2*-CH_2-CH_2-CH_3), 2.65 (2H, CO-CH-*CH_2*-CO), 2.44 (4H, NH-CH_2-CH_2-CH_2-N(*CH_2*CH_3)$_2$), 2.37 (2H, NH-CH_2-CH_2-*CH_2*-N(CH_2CH_3)$_2$), 1.53 (2H, NH-CH_2-*CH_2*-CH_2-N(CH_2CH_3)$_2$), 1.38 (2H, NH-CH_2-*CH_2*-CH_2-CH_3), 1.24 (2H, NH-CH_2-CH_2-*CH_2*-CH_3), 0.93 (6H, NH-CH_2-CH_2-CH_2-N(CH_2*CH_3*)$_2$), 0.84 (3H, NH-CH_2-CH_2-CH_2-*CH_3*); FTIR (KBr) [cm^{-1}]: 3313 (νNH amide), 2965 ($\nu_{as}CH_3$), 2935 ($\nu_{as}CH_2$), 1648 (amide I), 1541 (amide II).

Fluorescent marking was used to determine the dissolution rate of the matrix at the pH of the oral cavity (pH = 6.8). The modification of PSI with *L*-tryptophan methyl ester in 1 mol% was done in the same way as reported earlier [36]. Further steps were carried out in the same way as for the non-marked polymer DEP50B50. The fluorescent polymer is designated as T1DEP50B49.

2.2.2. Fabrication of electrospun matrices

Solutions of DEP50B50 in ethanol were prepared at various concentrations (20, 25 and 30 wt%) for electrospinning, with the resulting matrices denoted as M20, M25 and M30. A homemade electrospinning instrument equipped with a high voltage DC supply (MA 2000 NT-35) was used to electrospin the DEP50B50 polymer. A grounded plate covered with aluminum foil was used as collector. The applied voltage was 20 kV, and the distance of the spinneret from the collector was 15 cm in each case. The polymer solutions were filled in a syringe and dosed by a syringe pump (Harvard Apparatus). The volume rate was set to 0.5 ml h^{-1}. The product was a white, thin, random mesh. The experiments were carried out at ambient temperature and the relative humidity was 50%. The same conditions were applied during storage of the matrices.

In vitro matrix dissolution and drug release in simulated salivary fluid (pH = 6.8) were studied by using the fluorescently marked polymer (T1DEP50B49) [36] and vitamin B_{12} as a model drug. Prior to electrospinning, 5 mg of vitamin B_{12} was dissolved in 0.71 g solution of T1DEP50B49 (25 wt% polymer in ethanol). The matrices were prepared in the same way as those without the drug. 10 mg of the final solid matrix contained 250 μg vitamin B_{12}.

Besides the electrospun matrices, free films were prepared by evaporation of the ethanol from their solutions. The given solution was poured onto a glass plate bordered with a 1 mm thick silicone frame. The coated plate was dried at room temperature for 48 h under 50% relative humidity. Finally, the film was peeled off from the substrate. The concentration of the polymer was 25 wt% in its ethanol solution, while in the drug release study the final concentration of vitamin B_{12} in the solid film was the same as in the electrospun matrices.

2.3. Characterization

2.3.1. Physico-chemical characterization

^{1}H NMR spectra of the polymers were recorded using a Bruker 500 MHz spectrometer with 128 scans in DMSO-d_6 (3 wt% polymer solution). TMS (0.03 vol%) was used as internal standard. FTIR spectra were recorded using a Bruker Tensor 27 FTIR spectrometer on KBr pellets (1.5 mg polymer or fibrous matrix/250 mg KBr) from 4000 to 400 cm^{-1} with 128 scans and a resolution of 2 cm^{-1} for each sample. The density of the dry polyaspartamide, DEP50B50 was determined by helium pycnometry (Ultrapycnometer 1000, Quantachrome). This value was used for the calculation of the specific surface area (SSA) of the resulting matrices (Supplementary Data).

The polymer solutions were characterized by measuring their viscosity, surface tension and conductivity. DEP50B50 was dissolved in ethanol at concentrations of 15, 20, 25, 30 and 35 wt%. The viscosity of the polymer solutions was determined with a rolling ball viscometer (Lovis 2000, Anton Paar) coupled with a density meter (DMA 4500 M, Anton Paar). The viscosity measurements were carried out at an angle of 45°. The diameters of the capillary and the ball used were 1.59 mm and 1.5 mm, respectively. The surface tension of the solutions was determined by using a drop shape analysis system (DSA-30, Kruss). A pendant droplet of the solution was formed at the end of a syringe fixed vertically, and an image was taken at the moment when the drop snapped from the apex of the syringe. The surface tension was calculated from the shape of the drop as described elsewhere [33]. A conductometer (inoLab Level 2, WTW) equipped with a conductivity cell (Tectracon 325, WTW) was used to determine the specific conductivity of the polymer solutions at 25 °C.

2.3.2. Scanning electron microscopy

The morphology of the samples was investigated with a Carl Zeiss Merlin field-emission high-resolution scanning electron microscope (SEM). A conducting layer with a thickness of 15 nm was applied by cathode sputtering using a (80/20) Au/Pd alloy. Images were recorded with 5 kV accelerating voltage (300 pA). The characteristic size of the fibers was determined by JMicroVision V.1.2.7 image analysis software, the average value was calculated from at least 200 fibers per sample. Calculation of the specific surface area (SSA) of the matrices can be found in the Supplementary Data.

2.3.3. Thermal analysis (TGA, DSC) and X-ray diffraction (XRD)

Thermogravimetric analysis of the DEP50B50 polymer and the matrices was carried out with a PerkinElmer Simultaneous Thermal Analyser. Samples of about 10 mg were heated from 30 to 600 °C at a scanning rate of 10 °C min^{-1} under N_2 atmosphere.

The glass transition temperature (T_g) of the matrices was determined by differential scanning calorimetry (DSC). DSC traces were recorded with a PYRIS Diamond Differential Scanning Calorimeter (PerkinElmer). Two heating and one cooling run were performed on 10 mg samples in N_2 atmosphere with a heating and cooling rate of 10 °C min^{-1} between −60 and 120 °C. The first heating-cooling cycle was used to erase the thermal history and remove residual organic solvent as well as moisture. DSC curves recorded in the second heating run were used to determine the T_g of the samples.

Powder XRD patterns were measured by a PANalytical X'pert Pro MPD X-ray diffractometer (Malvern Panalytical Ltd.) using Cu Kα radiation (α1 = 1.5406 λ, α2 = 1.5444 λ). Each sample was scanned at 40 kV and 30 mA in the 2Θ interval 5–65° at scanning rate 0.1°/s with step size 0.010°.

2.3.4. Matrix dissolution and drug release studies

A piece of the drug loaded matrix (10 mg) was immersed in 20 ml of SSF (pH = 6.8, T = 37 °C). The measurements were carried out in a continuously stirred vessel (V = 50 ml, stirring rate: 200 rpm, Fig. S1, Supplementary Data). Samples of 2 ml were taken at predetermined time intervals, and replaced with 2 ml fresh SSF. The experiment was performed in triplicate, and the averaged results were used for evaluation. The amount of dissolved T1DEP50B49 was determined by fluorescence spectroscopy (PerkinElmer LS55 fluorescence spectrometer; λ_{ext}: 270 nm; λ_{em}: 350 nm). The concentration of released vitamin B_{12} was measured by UV–Vis spectrophotometry (Jena Specord 200 UV–Vis spectrophotometer, λ_{abs} = 361 nm [48], Fig. S2, Supplementary Data). Dissolution rate constant of the polyaspartamides at given pH was calculated by the Noyes–Whitney equation [49], (1):

$$\left(\frac{c_t}{c_\infty}\right) = 1 - e^{-kt} \tag{1}$$

where c_t is the concentration of the dissolved polymer at time t and c_∞ is the concentration of the dissolved polymer at infinite time (20 min in our experiments), k is the dissolution rate constant. The Noyes–Whitney

equation was also applied to describe the drug release profiles.

Results of the dissolution and release tests were analyzed statistically with GraphPad Prism software (version 5). Two-way ANOVA (with Bonferroni post-tests) analysis was applied. The results are expressed as mean values ± standard deviation (SD). A level of $p \leq 0.05$ was taken as significant, $p \leq 0.01$ as very significant, and $p \leq 0.001$ as highly significant.

3. Results and discussion

3.1. Effect of the polymer composition

Our aim was to prepare electrospun matrices of polyaspartamides that provide rapid drug release in the oral cavity. Ethanol was chosen as a green and pharmaceutically accepted solvent [13], as an alternative to the toxic or hazardous solvents often used in electrospinning. Polar drug molecules with low aqueous solubility are often soluble and stable in ethanol [50], which has a relatively high dielectric constant and evaporates easily [8]. However, the use of ethanol with no additives for electrospinning has been reported only for a limited number of polymers [9,18–24]. Polyaspartamides were prepared by modifying PSI with dialkylaminoalkyl [2-(dimethylamino)ethyl, 2-(diethylamino) ethyl, 3-(dimethylamino)propyl, 3-(diethylamino)propyl] groups to introduce cationic character into the polymer. The presence of dialkylaminoalkyl side groups ensures good solubility of the polyaspartamides in ethanol and in water over a wide pH range (pH 1–9) [36]. The large specific surface area (1–10 $m^2\ g^{-1}$) facilitates the moisture uptake of the matrices, which can be reduced by introducing alkyl side groups. Accordingly, the polymers were modified with alkyl side groups (*n*-propyl, *n*-butyl, *n*-hexyl), in addition to cationic groups, to control the solubility and water uptake. The type and molar ratio of different side groups was selected by electrospinning of the polymer solutions and by the examination of the matrices produced (Fig. 1). The size of the fibers formed from polymers with *n*-propyl side groups varied over a wide range, while the aqueous solubility of the matrices prepared from polyaspartamides containing *n*-hexyl ligands was poor (Fig. 1d); for this reason *n*-butyl side groups were used in further experiments. Polyaspartamides containing more than 75 mol% of alkyl side groups were poorly soluble at the pH of saliva (pH = 6.8), and moisture uptake decreased, but fibers stuck together and beads were observed (Fig. 1b). The type of cationic groups also had a significant effect on fiber formation and moisture uptake. Increasing the alkylene chain length from ethylene (DME, DEE) to propylene (DMP, DEP) the fiber formation improved. Fibers formed with smaller size (diameter or width and thickness) and narrower size distribution (Fig. 1a). Moisture uptake of the matrix decreased with increasing the chain length of *N*-alkyl side groups (Fig. 1c) but matrices prepared from polyaspartamides containing more than 50 mol% (dimethylamino)alkyl side group (DME, DMP) or more than 75 mol% (diethylamino)alkyl side group (DEE, DEP) were hygroscopic, which makes their storage difficult. Finally, polyaspartamide containing 50 mol% DEP and 50 mol% B groups (DEP50B50) was selected, as this polymer forms fibers in the range of a few hundred nanometers from which fast dissolution was expected.

The chemical structure of PSI and DEP50B50 was confirmed by ^{1}H NMR (Fig. S3, Supplementary Data) and FTIR spectroscopy. The results of MTT proliferation assay performed on PC3 cells (Fig. S4, Supplementary Data), along with our study on the biocompatibility of cationic polyaspartamides [43], are in support of human biological use of DEP50B50.

3.2. Preparation of DEP50B50 fibers

According to the literature data and our results, fiber formation strongly depends on the chemical structure of the polymer [12]. The morphology of the prepared fibers also depends on the properties of the polymer solution, especially the viscosity, the surface tension and the conductivity [6]. These characteristics were determined over a wide concentration range to find the optimal composition of the polymer solution for electrospinning (Fig. 2).

The accelerating force of the electric field must permanently overcome the force arising from the surface tension of the solution to obtain fibrous morphology. The surface tension of the solution remains practically unchanged with increasing the polymer concentration (Fig. 2a) and is similar to that of the solvent (21.9 mN m^{-1}) [20]. Only a very slight increase was observed at large concentrations, and hence the polymer can be considered as capillary-inactive in ethanol. Similar behavior was observed for another polyamide type polymer, nylon 6 in formic acid [51]. The viscosity and conductivity depend strongly on the

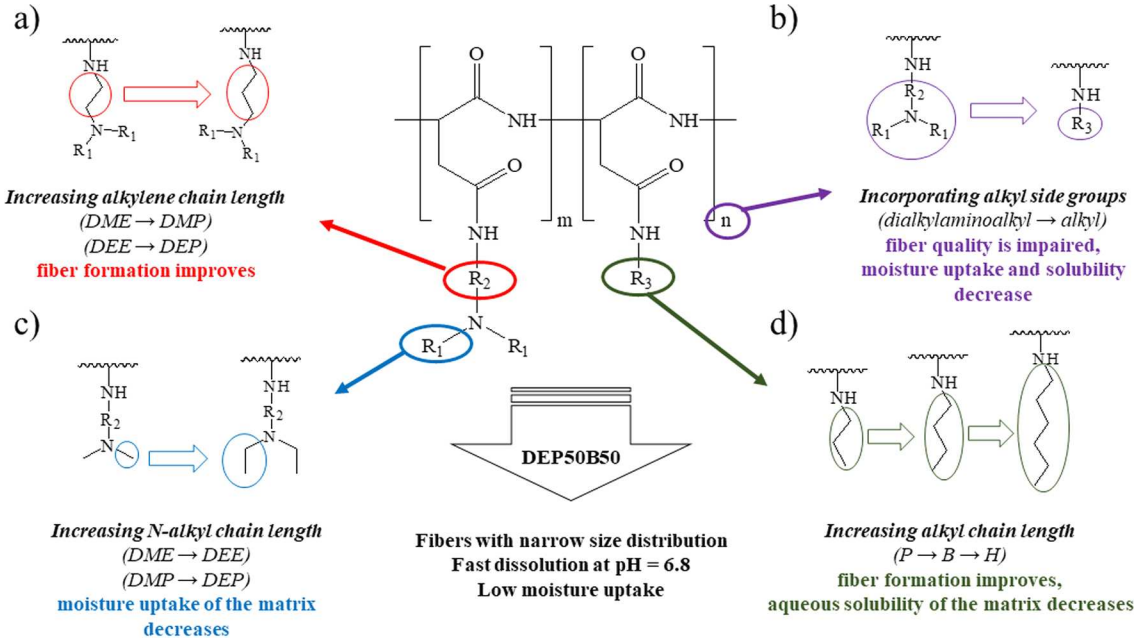

Fig. 1. Effect of the polymer composition on the fiber formation and the properties of the electrospun matrices: (a) increasing alkylene chain length, (b) incorporating alkyl side groups, (c) increasing *N*-alkyl chain length, (d) increasing alkyl chain length.

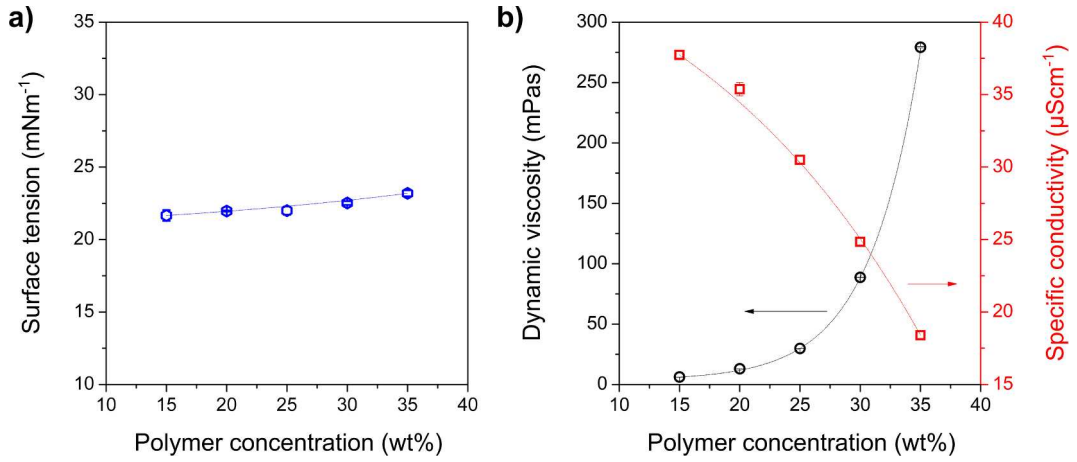

Fig. 2. (a) Surface tension and (b) dynamic viscosity and specific conductivity of the ethanol solutions as a function of the DEP50B50 concentration (curves are to guide the eye).

concentration of the polymer (Fig. 2b). The lowest concentration and corresponding dynamic viscosity suitable for electrospinning were found to be 20 wt% and 13 mPas, respectively. The large specific conductivity at 15 wt% concentration should lead to jet formation [12], but the polymer fibers broke into droplets before reaching the collector because of the low viscosity and incomplete solvent evaporation. Increasing the concentration of the DEP50B50 polymer to 20, 25 or 30 wt % increases the viscosity of the solution, thereby making the electrospinning feasible, thus fibrous matrices were electrospun. At 35 wt% concentration, however, fibers did not form owing to the decreased conductivity, since the electrostatic force exerted by the electric field is insufficient to overcome the forces from the surface tension and the greatly increased dynamic viscosity (35 wt%, 279 mPas). Although the conductivity can be increased by adding inorganic salts, we did not perform additional experiments at high polymer concentrations, since the use of an additive requires an undesirable removal step after fiber formation. As a result, in the subsequent experiments, DEP50B50 ethanol solutions with polymer concentrations between 20 and 30 wt% were used for electrospinning. The voltage of 20 kV and the flow rate of 0.5 ml h^{-1} were found to be appropriate for preparing fibers in the chosen concentration range. Details of the electrospinning and the solution parameters are listed in Table 1.

3.3. Characterization of the electrospun fibers

3.3.1. Morphology

The size and shape of the fibers vary considerably with polymer concentration, as shown in Fig. 3. Nanofibers electrospun from 20 wt% solution (M20) are stuck together and contain beads (Fig. 3a). This can be explained by incomplete evaporation of the solvent before the polymer reaches the surface of the collector [6]. Although the specific surface area of the M20 fibers is found to be quite large (9.4 m^2 g^{-1}, Table 1), the size distribution of the fiber diameter is rather wide [PDI: 0.22 (PDI: polydispersity index of fiber diameter, Supplementary Data)] and cylindrical fiber diameter varies between 100 nm and 1 μm (Fig. 3a). Electrospinning from a 25 wt% solution yielded ribbon-like fibers without beads having a submicron size with a narrow size distribution of the fiber thickness (mean size, d = 335 ± 71 nm, PDI = 0.02) and width (d = 743 ± 112 nm, PDI = 0.04) (Fig. 3b). The ribbon-like shape of the fibers can be explained by various factors, such as the high vapor pressure of the solvent employed (ethanol in the present case) [52], while the shape also depends on the polymer concentration, or on the structure of the polymer itself [52–54]. The specific surface area calculated (7.7 m^2 g^{-1}, Table 1.) remained sufficiently large to provide rapid dissolution of the M25 matrix in an

Table 1
Details of the preparation and the morphological properties of DEP50B50 fibers.

Sample code	c[a] (wt%)	ρ[b] (g cm^{-3})	η[c] (*m*Pas)	γ[d] (*m*Nm^{-1})	κ[e] (μS cm^{-1})	U[f] (kV)	$\dot{V}$[g] (ml h^{-1})	r[h] (cm)	d[i] (nm)		SSA[j] (m^{2}g^{-1})	T$_g$[k] (°C)
									width	thickness		
M15	15	0.830	6	21.7	37.7	20	0.5	15	–		–	–
M20	20	0.844	13	22.0	35.4	20	0.5	15	397 ± 179 (cylindrical fibers)		9.4	48
M25	25	0.859	30	22.0	30.5	20	0.5	15	743 ± 112	335 ± 71 (ribbons)	7.7	49
M30	30	0.876	89	22.5	24.8	20	0.5	15	1728 ± 294	1007 ± 171 (ribbons)	2.8	51
M35	35	0.893	279	23.2	18.4	20	0.5	15	–		–	–

[a] Concentration.
[b] Density.
[c] Dynamic viscosity.
[d] Surface tension.
[e] Specific conductivity of the DEP50B50 ethanol solutions at 25 °C.
[f] Applied voltage.
[g] Flow rate.
[h] Distance between the spinneret and the collector.
[i] Size (diameter or width and thickness) of the fibers with standard deviation.
[j] Specific surface area of the matrices, $\rho_{DEP50B50}$ = 1.12 g cm^{-3}.
[k] Glass transition temperature.

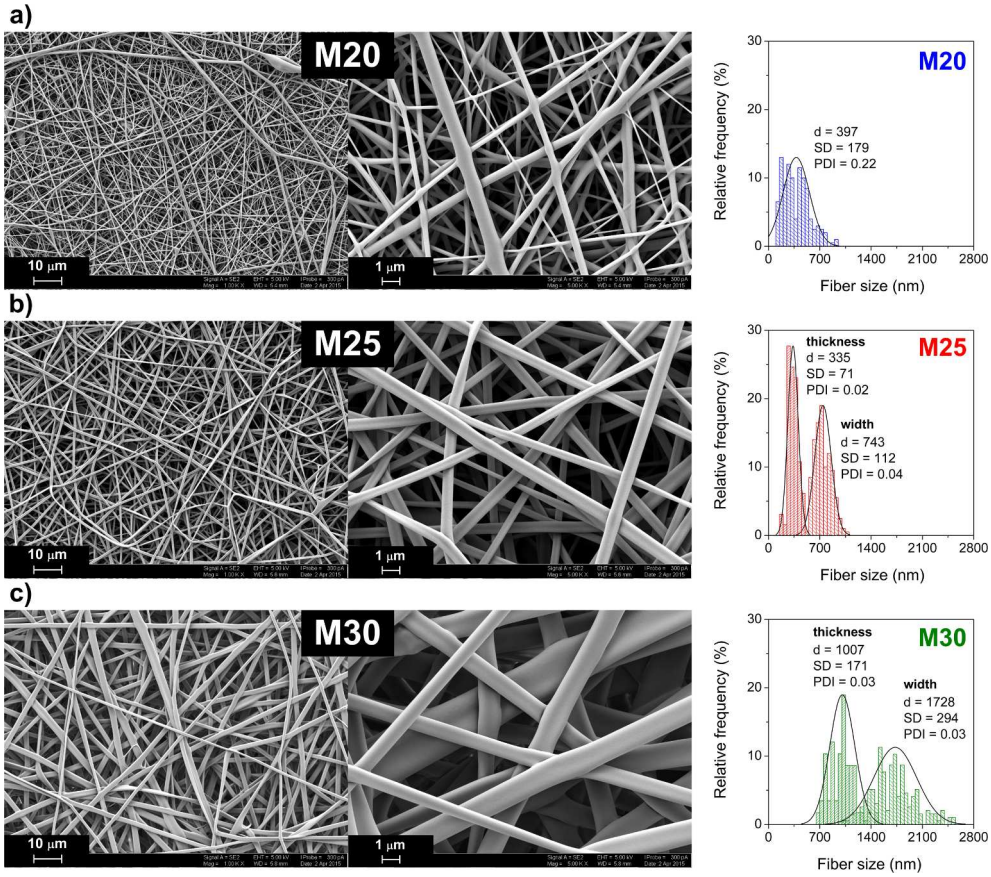

Fig. 3. SEM micrographs and fiber size distribution of matrices electrospun from DEP50B50 ethanol solutions at concentrations of (a) 20 wt% (M20), (b) 25 wt% (M25) and (c) 30 wt% (M30), respectively.

appropriate solvent. Fibers electrospun from a 30 wt% solution (M30) also display ribbon-like morphology, but the thickness (d = 1007 ± 171 nm) and the width (d = 1728 ± 294 nm) of the fibers are larger than in the previous case (Fig. 3c). The increase in size can be explained by the high viscosity and the reduced specific conductivity (Fig. 2b). This microfibrous morphology yields a decreased specific surface area (2.8 m^2 g^{-1}, Table 1). In conclusion, 25 wt% was found to be the ideal concentration of the DEP50B50 and T1DEP50B49 polymers for preparing fibers in the submicron size range with a narrow size distribution. It is important to emphasize that, contrary to examples reported in the literature [53], the matrices were prepared with no additives. This can be explained by the high dielectric constant of the solvent, which prevents the formation of beads [55].

3.3.2. Stability and thermal properties

FTIR spectroscopy was used to characterize the effect of electrospinning on the chemical structure of the DEP50B50 polymer. Fig. 4a presents the FTIR spectra of the DEP50B50 polymer and the prepared M25 matrix. IR bands assigned to the polymer backbone (amide I.: 1648 cm^{-1}, amide II.: 1541 cm^{-1}) and to the side groups of DEP50B50 (νCH_2: 2935 cm^{-1}, νCH_3: 2965 cm^{-1}) attest to the presence of all the expected functional groups. Additionally, the characteristic absorption band of the imide ring at around 1718 cm^{-1} is not present in the spectra of polyaspartamides, proving that ring-opening of the succinimide repeating units was complete [36]. More importantly, the two spectra match each other perfectly, showing that the polymer does not suffer chemical degradation during electrospinning.

The thermal decomposition of the DEP50B50 and the M25 matrix was determined in the temperature range from 30 to 600 °C by

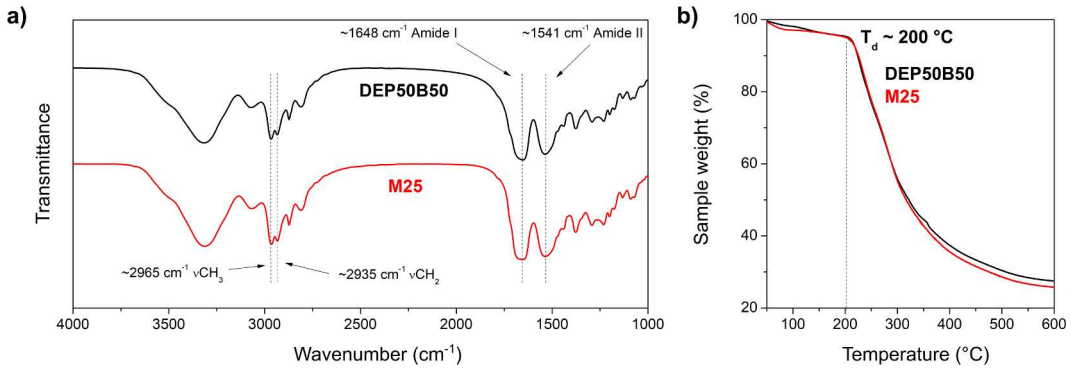

Fig. 4. (a) FTIR spectra and (b) TGA curves of the DEP50B50 polymer and the M25 matrix.

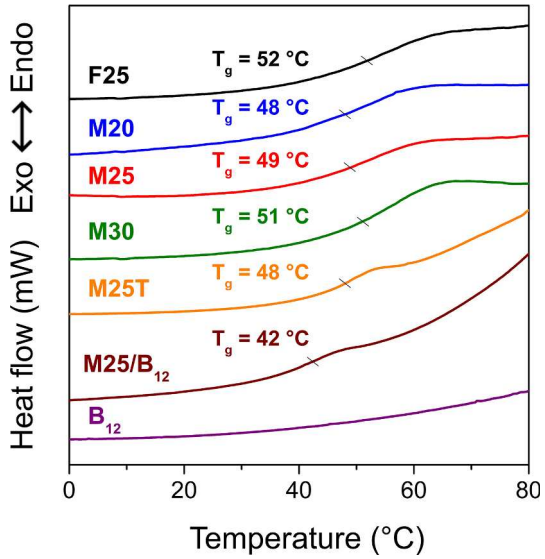

Fig. 5. DSC traces of DEP50B50 film (F25), DEP50B50 matrices (M20, M25, M30), a matrix made of T1DEP50B49 (M25T), DEP50B50 matrix loaded with vitamin B_{12} (M25/B_{12}), and the pure vitamin B_{12} (B_{12}).

thermogravimetric analysis (TGA). Weight loss occurs below 100 °C due to the elimination of solvents (residual ethanol, absorbed water, ~5–6 wt%). Both the polymer and the electrospun matrix decompose around 200 °C (Fig. 4b). This relatively high thermal decomposition temperature (T_d) enables to process these polymers at high temperatures. For instance, the matrix can be sterilized using dry heat (commonly carried out in the temperature range of 160–180 °C), or polymer processing by melt extrusion or melt electrospinning can be also feasible without chemical decomposition.

DSC measurements were made on the electrospun matrices (M20, M25, M30) and on a free film prepared from DEP50B50 (F25) and compared to each other (Fig. 5). As a reference, the DSC trace of vitamin B_{12} (B_{12}) is also plotted indicating the absence of any peak or step in the temperature range of 0–80 °C. The glass transition temperature (T_g) of the polymers is detected in the temperature range of 48–52 °C for both the free film and the fibrous matrices. A slight suppression of T_g with decreasing fiber diameter (and increasing specific surface area) was observed, which result corresponds to the theoretical and the experimental predictions of the literature [56,57]. Nevertheless, large size-dependent suppression in the T_g is typical in the case of polymer fibers with smaller diameter. In our case, the electrospinning does not have a significant effect on the T_g. The almost identical T_g of the M25T and M25 matrices prove that fluorescent marking does not affect glass transition temperature either. However, the T_g of the M25 matrix containing B_{12} (M25/B_{12}) was slightly lower than that of the M25 matrix, but considering the wide temperature range of the glass transition the difference is not significant. Since the glass transition temperature of the electrospun matrices is higher than the room temperature (~50 °C), the matrices are in glassy state, i.e., the motion of chain segments is frozen at room temperature. The glassy state can hinder the crystallization of the loaded material, which is important for the future application of the matrix in the formulation of crystalline drugs.

X-ray diffraction is generally used to analyze the prepared matrices with respect to the crystallinity of the polymer and the loaded drug. In consistency with the results of the thermal analysis, no reflection peaks of a crystalline phase could be observed in the diffractograms (Fig. S5, Supplementary Data), demonstrating that the vitamin B_{12}, the pure DEP50B50 matrix, and the matrix loaded with the model drug are amorphous. This property can ensure the fast dissolution of the matrix and rapid release of the model drug.

3.3.3. Matrix dissolution and drug release

Fast dissolution of the matrix is required to exploit the advantage of sublingual and buccal drug delivery. The dissolution profile of the T1DEP50B49 polyaspartamide matrix and the release of vitamin B_{12} were determined at the pH of saliva (6.8) and at physiological temperature (37 °C). T1DEP50B49 as a polymer labeled with fluorescent tryptophan methyl ester was used to monitor the dissolution of the matrix. This method was applied successfully earlier for poly(aspartic acid) derivatives with alkyl side groups [35] and cationic polyaspartamides [36]. We chose vitamin B_{12} as a model drug for several reasons: a) it is soluble in ethanol (≥1 g/L) [58], the solvent we used for electrospinning, b) vitamin B_{12} has high aqueous solubility (12–14 g/L) [59], c) its detection is easy by UV–VIS spectroscopy, and d) oral administration of vitamin B_{12} (including sublingual) is widespread, especially in the treatment of vitamin B_{12} deficiency [60]. As vitamin B_{12} is highly soluble in saliva and typically used in very low, 1–1000 μg, doses in the formulations [60], the role of the polymer matrix is to facilitate the handling of the active compound for both the production and the patients as well as to ensure rapid release of incorporated vitamin B_{12}. Vitamin B_{12} was incorporated in the fibers during electrospinning (see photo in Fig. 6a of a T1DEP50B49 matrix loaded with vitamin B_{12}). As noted in Fig. 6b, more than 82% of the T1DEP50B49 matrix (M25T) was dissolved, while 90% of vitamin B_{12} ($B_{12,M}$) was released in the first minute of the experiment, indicating that the fast dissolution of the matrix (k_{M25T} = 2.2 min^{-1}) is accompanied by the rapid release of vitamin B_{12} ($k_{B12,M}$ = 2.5 min^{-1}) incorporated. To characterize the effect of formulation on the release of vitamin B_{12}, the dissolution profile of the pure vitamin B_{12} (B_{12}) and the release of vitamin B_{12} incorporated in a T1DEP50B49 film ($B_{12,F}$) were also determined at the pH of saliva (pH = 6.8). As shown in Fig. 6c, there is no significant difference between the dissolution profile of the pure vitamin B_{12} (B_{12}) and the release profile of vitamin B_{12} incorporated in the nanofibrous matrix ($B_{12,M}$) ($p > 0.05$). However, the

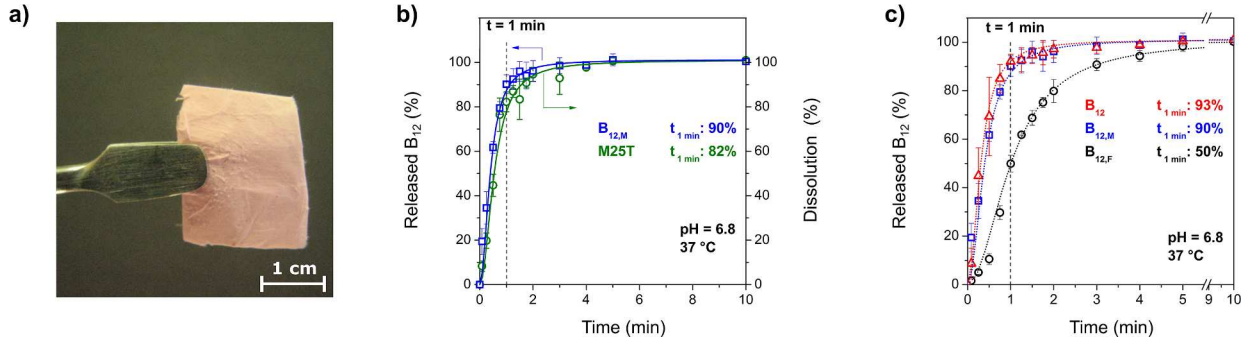

Fig. 6. (a) Photograph of the T1DEP50B49 matrix loaded with vitamin B_{12} (M25T/B_{12}), (b) dissolution of the T1DEP50B49 matrix (M25T) and rapid release of vitamin B_{12} from this matrix ($B_{12,M}$), and (c) dissolution profile of the pure vitamin B_{12} (B_{12}), and release profiles of vitamin B_{12} from T1DEP50B49 matrix ($B_{12,M}$) and T1DEP50B49 film ($B_{12,F}$) (SSF, pH = 6.8, 37 °C).

release of vitamin B_{12} entrapped in a film ($B_{12,F}$) was significantly slower than that from the T1DEP50B49 matrix ($B_{12,M}$) ($p < 0.001$, highly significant) over the entire time range. B_{12} and $B_{12,M}$ dissolves almost completely (≥90%) within one minute, while release of $B_{12,F}$ is only just above 50% in that time. Dissolution rate constants calculated by the Noyes–Whitney equation (Eq. (1)) are in agreement with this observation (k_{B12} = 2.6 min^{-1}, $k_{B12,M}$ = 2.5 min^{-1}, $B_{12,F}$ = 1.6 min^{-1}).

4. Conclusion

Nanofibrous matrices were successfully prepared from a cationic polyaspartamide containing 50 mol% 3-(diethylamino)propyl and 50 mol% *n*-butyl side groups by solvent electrospinning using ethanol, a green and pharmaceutically accepted solvent (ICH 3 Class solvent). Matrices were produced with no additives, and submicron sized fibers with a narrow size distribution were achieved with a polymer concentration of 25 wt%. Both the polymer and the fibrous matrices have a high thermal decomposition temperature (200 °C) and a glass transition temperature at around 50 °C. The matrix dissolved almost completely within one minute in simulated salivary fluid (pH = 6.8), which was accompanied by the rapid release of vitamin B_{12} incorporated. These results suggest the potential application of electrospun matrices of polyaspartamides in sublingual and buccal drug delivery.

5. Data availability statement

The raw/processed data required to reproduce these findings cannot be shared at this time as the data also forms part of an ongoing study.

CRediT authorship contribution statement

Csaba Németh: Conceptualization, Methodology, Investigation, Formal analysis, Writing - original draft. **Benjámin Gyarmati:** Conceptualization, Methodology, Writing - review & editing. **Jenő Gacs:** Investigation. **Diana V. Salakhieva:** Investigation. **Kolos Molnár:** Methodology, Resources, Writing - review & editing. **Timur Abdullin:** Resources, Writing - review & editing, Funding acquisition. **Krisztina László:** Writing - review & editing, Funding acquisition. **András Szilágyi:** Conceptualization, Methodology, Resources, Writing - review & editing, Supervision, Funding acquisition.

Acknowledgement

This research was supported by the National Research, Development and Innovation Office (NKFIH FK 125074) and the FP7-PEOPLE-2010-IRSES269267 (Marie Curie International Research Staff Exchange Scheme) project is acknowledged. B. Gyarmati and K. Molnár acknowledges the financial support of the János Bolyai Research Scholarship of the Hungarian Academy of Sciences. A. Szilágyi is grateful for the support of the ÚNKP-17-4-III New National Excellence Program of the Ministry of Human Capacities. Timur Abdullin acknowledges the support of the Russian Government Program of Competitive Growth for Kazan Federal University. We thank Emőke Albert (Department of Physical Chemistry and Materials Science, Budapest University of Technology and Economics, BME) for helping in the surface tension measurements and Imre Miklós Szilágyi (Department of Inorganic and Analytical Chemistry, BME) for helping in the XRD measurements, along with Viacheslav Vorobev and Yury Osin (Interdisciplinary Center for Analytical Microscopy, Kazan Federal University) for performing the SEM analysis.

Appendix A. Supplementary data

Supplementary data to this article can be found online at https://doi.org/10.1016/j.eurpolymj.2020.109624.

References

[1] T. Goswami, A. Kokate, B.R. Jasti, X. Li, In silico model of drug permeability across sublingual mucosa, Arch. Oral Biol. 58 (2013) 545–551, https://doi.org/10.1016/j.archoralbio.2012.09.020.
[2] M. Sattar, O.M. Sayed, M.E. Lane, Oral transmucosal drug delivery – current status and future prospects, Int. J. Pharm. 471 (2014) 498–506, https://doi.org/10.1016/j.ijpharm.2014.05.043.
[3] P. Vrbata, P. Berka, D. Stránská, P. Doležal, M. Musilová, L. Čižinská, Electrospun drug loaded membranes for sublingual administration of sumatriptan and naproxen, Int. J. Pharm. 457 (2013) 168–176, https://doi.org/10.1016/j.ijpharm.2013.08.085.
[4] J.L. Manasco, C. Tang, N.A. Burns, C.D. Saquing, S.A. Khan, Rapidly dissolving poly (vinyl alcohol)/cyclodextrin electrospun nanofibrous membranes, RSC Adv. 4 (2014) 13274–13279, https://doi.org/10.1039/c3ra43836h.
[5] E. Borbás, A. Balogh, K. Bocz, J. Müller, É. Kiserdei, T. Vigh, B. Sinkó, A. Marosi, A. Halász, Z. Dohányos, L. Szente, G.T. Balogh, Z.K. Nagy, In vitro dissolution-permeation evaluation of an electrospun cyclodextrin-based formulation of aripiprazole using μFlux™, Int. J. Pharm. 491 (2015) 180–189, https://doi.org/10.1016/j.ijpharm.2015.06.019.
[6] X. Zong, K. Kim, D. Fang, S. Ran, B.S. Hsiao, B. Chu, Structure and process relationship of electrospun bioabsorbable nanofiber membranes, Polymer 43 (2002) 4403–4412, https://doi.org/10.1016/S0032-3861(02)00275-6.
[7] D.S. Katti, K.W. Robinson, F.K. Ko, C.T. Laurencin, Bioresorbable nanofiber-based systems for wound healing and drug delivery: optimization of fabrication parameters, J. Biomed. Mater. Res. - Part B Appl. Biomater. 70 (2004) 286–296, https://doi.org/10.1002/jbm.b.30041.
[8] N. Bhardwaj, S.C. Kundu, Electrospinning: a fascinating fiber fabrication technique, Biotechnol. Adv. 28 (2010) 325–347, https://doi.org/10.1016/j.biotechadv.2010.01.004.
[9] Z.K. Nagy, A. Balogh, B. Vajna, A. Farkas, G. Patyi, Á. Kramarics, G. Marosi, Comparison of electrospun and extruded soluplus®-based solid dosage forms of improved dissolution, J. Pharm. Sci. 101 (2012) 322–332, https://doi.org/10.1002/jps.22731.
[10] Z.K. Nagy, A. Balogh, B. Démuth, H. Pataki, T. Vigh, B. Szabó, K. Molnár, B.T. Schmidt, P. Horák, G. Marosi, G. Verreck, I. Van Assche, M.E. Brewster, High speed electrospinning for scaled-up production of amorphous solid dispersion of itraconazole, Int. J. Pharm. 480 (2015) 137–142, https://doi.org/10.1016/j.ijpharm.2015.01.025.
[11] Z.M. Huang, Y.Z. Zhang, M. Kotaki, S. Ramakrishna, A review on polymer nanofibers by electrospinning and their applications in nanocomposites, Compos. Sci. Technol. 63 (2003) 2223–2253, https://doi.org/10.1016/S0266-3538(03)00178-7.
[12] T.J. Sill, H.A. von Recum, Electrospinning: applications in drug delivery and tissue engineering, Biomaterials. 29 (2008) 1989–2006, https://doi.org/10.1016/j.biomaterials.2008.01.011.
[13] European Medicines Agency, ICH guideline Q3C (R7) on impurities: guideline for residual solvents, 44 (2018).
[14] J. Nam, Y. Huang, S. Agarwal, J. Lannutti, Materials selection and residual solvent retention in biodegradable electrospun fibers, J. Appl. Polym. Sci. 107 (2008) 1547–1554, https://doi.org/10.1002/app.27063.
[15] A. Balogh, G. Drávavölgyi, K. Faragó, A. Farkas, T. Vigh, P.L. Sóti, I. Wagner, J. Madarász, H. Pataki, G. Marosi, Z.K. Nagy, Plasticized drug-loaded melt electrospun polymer mats: characterization, thermal degradation, and release kinetics, J. Pharm. Sci. 103 (2014) 1278–1287, https://doi.org/10.1002/jps.23904.
[16] S. Yoshioka, V.J. Stella, Stability of Drugs and Dosage Forms, Kluwer Academic Publishers, 2002, https://doi.org/10.1007/b114443.
[17] C. Capello, U. Fischer, K. Hungerbühler, What is a green solvent? A comprehensive framework for the environmental assessment of solvents, Green Chem. 9 (2007) 927–934, https://doi.org/10.1039/b617536h.
[18] T. Maeda, K. Hagiwara, S. Yoshida, T. Hasebe, A. Hotta, Preparation and characterization of 2-methacryloyloxyethyl phosphorylcholine polymer nanofibers prepared via electrospinning for biomedical materials, J. Appl. Polym. Sci. 131 (2014) 40606, https://doi.org/10.1002/app.40606.
[19] T. Casian, E. Borbás, K. Ilyés, B. Démuth, A. Farkas, Z. Rapi, C. Bogdan, S. Iurian, V. Toma, R. Știufiuc, B. Farkas, A. Balogh, G. Marosi, I. Tomuță, Z.K. Nagy, Electrospun amorphous solid dispersions of meloxicam: influence of polymer type and downstream processing to orodispersible dosage forms, Int. J. Pharm. 569 (2019) 118593, https://doi.org/10.1016/j.ijpharm.2019.118593.
[20] S. Chuangchote, T. Sagawa, S. Yoshikawa, Electrospinning of poly(vinyl pyrrolidone): effects of solvents on electrospinnability for the fabrication of poly(p-phenylene vinylene) and TiO_2 nanofiber, J. Appl. Polym. Sci. 114 (2009) 2777–2791, https://doi.org/10.1002/app.30637.
[21] Y.H. Wu, D.G. Yu, H.C. Li, D.N. Feng, Electrospun nanofibers for fast dissolution of naproxen prepared using a coaxial process with ethanol as a shell fluid, Appl. Mech. Mater. 662 (2014) 29–32, https://doi.org/10.4028/www.scientific.net/amm.662.29.
[22] S. Kajdič, F. Vrečer, P. Kocbek, Preparation of poloxamer-based nanofibers for enhanced dissolution of carvedilol, Eur. J. Pharm. Sci. 117 (2018) 331–340, https://doi.org/10.1016/j.ejps.2018.03.006.
[23] J.Y. Park, I.H. Lee, G.N. Bea, Optimization of the electrospinning conditions for preparation of nanofibers from polyvinylacetate (PVAc) in ethanol solvent, J. Ind. Eng. Chem. 14 (2008) 707–713, https://doi.org/10.1016/j.jiec.2008.03.006.
[24] S. Shukla, E. Brinley, H.J. Cho, S. Seal, Electrospinning of hydroxypropyl cellulose fibers and their application in synthesis of nano and submicron tin oxide fibers, Polymer 46 (2005) 12130–12145, https://doi.org/10.1016/j.polymer.2005.10.

070.
[25] D.B. Khadka, D.T. Haynie, Protein- and peptide-based electrospun nanofibers in medical biomaterials, Nanomed. Nanotechnol. Biol. Med. 8 (2012) 1242–1262, https://doi.org/10.1016/j.nano.2012.02.013.
[26] D. Liang, B.S. Hsiao, B. Chu, Functional electrospun nanofibrous scaffolds for biomedical applications, Adv. Drug Deliv. Rev. 59 (2007) 1392–1412, https://doi.org/10.1016/j.addr.2007.04.021.
[27] M. Foox, M. Zilberman, Drug delivery from gelatin-based systems, Expert Opin. Drug Deliv. 12 (2015) 1547–1563, https://doi.org/10.1517/17425247.2015.1037272.
[28] K.R. Solomon, G.J.M. Velders, S.R. Wilson, S. Madronich, J. Longstreth, P.J. Aucamp, J.F. Bornman, Sources, fates, toxicity, and risks of trifluoroacetic acid and its salts: relevance to substances regulated under the Montreal and Kyoto Protocols, J. Toxicol. Environ. Heal. - Part B Crit. Rev. 19 (2016) 289–304, https://doi.org/10.1080/10937404.2016.1175981.
[29] O.D. Krishna, K.L. Kiick, Protein- and peptide-modified synthetic polymeric biomaterials, Biopolymers 94 (2010) 32–48, https://doi.org/10.1002/bip.21333.
[30] K. Molnar, D. Juriga, P.M. Nagy, K. Sinko, A. Jedlovszky-Hajdu, M. Zrinyi, Electrospun poly(aspartic acid) gel scaffolds for artificial extracellular matrix, Polym. Int. 63 (2014) 1608–1615, https://doi.org/10.1002/pi.4720.
[31] A. Jedlovszky-Hajdu, K. Molnar, P.M. Nagy, K. Sinko, M. Zrinyi, Preparation and properties of a magnetic field responsive three-dimensional electrospun polymer scaffold, Colloids Surf. A Physicochem. Eng. Asp. 503 (2016) 79–87, https://doi.org/10.1016/j.colsurfa.2016.05.036.
[32] C. Zhang, H. Li, Q. Yu, L. Jia, L.Y. Wan, Poly(aspartic acid) electrospun nanofiber hydrogel membrane-based reusable colorimetric sensor for Cu(II) and Fe(III) detection, ACS Omega 4 (2019) 14633–14639, https://doi.org/10.1021/acsomega.9b02109.
[33] S. Wang, X. Cao, M. Shen, R. Guo, I. Bányai, X. Shi, Fabrication and morphology control of electrospun poly(γ-glutamic acid) nanofibers for biomedical applications, Colloids Surf. B Biointerfaces 89 (2012) 254–264, https://doi.org/10.1016/j.colsurfb.2011.09.029.
[34] O.I. Kalaoglu-Altan, B. Verbraeken, K. Lava, T.N. Gevrek, R. Sanyal, T. Dargaville, K. De Clerck, R. Hoogenboom, A. Sanyal, Multireactive poly(2-oxazoline) nanofibers through electrospinning with crosslinking on the fly, ACS Macro Lett. 5 (2016) 676–681, https://doi.org/10.1021/acsmacrolett.6b00188.
[35] C. Németh, B. Gyarmati, T. Abdullin, K. László, A. Szilágyi, Poly(aspartic acid) with adjustable pH-dependent solubility, Acta Biomater. 49 (2017) 486–494, https://doi.org/10.1016/j.actbio.2016.11.065.
[36] C. Németh, D. Szabó, B. Gyarmati, A. Gerasimov, M. Varfolomeev, T. Abdullin, K. László, A. Szilágyi, Effect of side groups on the properties of cationic poly-aspartamides, Eur. Polym. J. 93 (2017) 805–814, https://doi.org/10.1016/j.eurpolymj.2017.02.024.
[37] E. Krisch, B. Gyarmati, A. Szilágyi, Preparation of pH-responsive poly(aspartic acid) nanogels in inverse emulsion, Period. Polytech. Chem. Eng. 61 (2017) 19–26, https://doi.org/10.3311/ppch.9788.
[38] E. Krisch, B. Gyarmati, D. Barczikai, V. Lapeyre, B.Á. Szilágyi, V. Ravaine, A. Szilágyi, Poly(aspartic acid) hydrogels showing reversible volume change upon redox stimulus, Eur. Polym. J. 105 (2018) 459–468, https://doi.org/10.1016/J.EURPOLYMJ.2018.06.011.
[39] B.Á. Szilágyi, Á. Némethy, A. Magyar, I. Szabó, S. Bősze, B. Gyarmati, A. Szilágyi, Amino acid based polymer hydrogel with enzymatically degradable cross-links, React. Funct. Polym. 133 (2018) 21–28, https://doi.org/10.1016/j.reactfunctpolym.2018.09.015.
[40] S.M. Thombre, B.D. Sarwade, Synthesis and biodegradability of polyaspartic acid: a critical review, J. Macromol. Sci. Part A - Pure Appl. Chem. 42 (2005) 1299–1315, https://doi.org/10.1080/10601320500189604.
[41] B.Á. Szilágyi, B. Gyarmati, G. Horvát, Á. Laki, M. Budai-Szűcs, E. Csányi, G. Sandri, M.C. Bonferoni, A. Szilágyi, The effect of thiol content on the gelation and mucoadhesion of thiolated poly(aspartic acid), Polym. Int. 66 (2017) 1538–1545, https://doi.org/10.1002/pi.5411.
[42] M. Budai-Szűcs, E.L. Kiss, B.Á. Szilágyi, A. Szilágyi, B. Gyarmati, S. Berkó, A. Kovács, G. Horvát, Z. Aigner, J. Soós, E. Csányi, Mucoadhesive cyclodextrin-modified thiolated poly(aspartic acid) as a potential ophthalmic drug delivery system, Polymers 10 (2018) 199, https://doi.org/10.3390/polym10020199.
[43] D. Salakhieva, V. Shevchenko, C. Németh, B. Gyarmati, A. Szilágyi, T. Abdullin, Structure–biocompatibility and transfection activity relationships of cationic poly-aspartamides with (dialkylamino)alkyl and alkyl or hydroxyalkyl side groups, Int. J. Pharm. 517 (2017) 234–246, https://doi.org/10.1016/j.ijpharm.2016.12.007.
[44] J.R. Moon, M.W. Kim, D. Kim, J.H. Jeong, J.H. Kim, Synthesis and self-assembly behavior of novel polyaspartamide derivatives for anti-tumor drug delivery, Colloid Polym. Sci. 289 (2011) 63–71, https://doi.org/10.1007/s00396-010-2307-6.
[45] J.R. Moon, Y.S. Jeon, D.J. Chung, D. Kim, J.-H. Kim, In Situ gelling and drug release behavior from novel temperature-sensitive polyaspartamides, Macromol. Res. 19 (2011) 515–518, https://doi.org/10.1007/s13233-011-0507-7.
[46] G. Pitarresi, F.S. Palumbo, C. Fiorica, F. Calascibetta, G. Giammona, Electrospinning of α, β-poly(N-2-hydroxyethyl)-DL-aspartamide-graft-polylactic acid to produce a fibrillar scaffold, Eur. Polym. J. 46 (2010) 181–184, https://doi.org/10.1016/j.eurpolymj.2009.09.001.
[47] D.K. Knight, E.R. Gillies, K. Mequanint, Biomimetic L-aspartic acid-derived functional poly(ester amide)s for vascular tissue engineering, Acta Biomater. 10 (2014) 3484–3496, https://doi.org/10.1016/j.actbio.2014.04.014.
[48] A. Samadi-Maybodi, S.K.H.N. Darzi, Simultaneous determination of vitamin B12 and its derivatives using some of multivariate calibration 1 (MVC1) techniques, Spectrochim. Acta - Part A Mol. Biomol. Spectrosc. 70 (2008) 1167–1172, https://doi.org/10.1016/j.saa.2007.10.037.
[49] A. Dokoumetzidis, V. Papadopoulou, P. Macheras, Analysis of dissolution data using modified versions of Noyes-Whitney equation and the Weibull function, Pharm. Res. 23 (2006) 256–261.
[50] U. Domañska, A. Pobudkowska, A. Pelczarska, P. Gierycz, pKa and solubility of drugs in water, ethanol, and 1-octanol, J. Phys. Chem. B 113 (2009) 8941–8947, https://doi.org/10.1021/jp900468w.
[51] Y.J. Ryu, H.Y. Kim, K.H. Lee, H.C. Park, D.R. Lee, Transport properties of electrospun nylon 6 nonwoven mats, Eur. Polym. J. 39 (2003) 1883–1889, https://doi.org/10.1016/S0014-3057(03)00096-X.
[52] S. Koombhongse, W. Liu, D.H. Reneker, Flat polymer ribbons and other shapes by electrospinning, J. Polym. Sci. Part B Polym. Phys. 39 (2001) 2598–2606, https://doi.org/10.1002/polb.10015.
[53] A. Greiner, J.H. Wendorff, Electrospinning: a fascinating method for the preparation of ultrathin fibers, Angew. Chemie - Int. Ed. 46 (2007) 5670–5703, https://doi.org/10.1002/anie.200604646.
[54] M. Dhanalakshmi, J.P. Jog, Preparation and characterization of electrospun fibers of Nylon 11, Express Polym. Lett. 2 (2008) 540–545, https://doi.org/10.3144/expresspolymlett.2008.65.
[55] C.J. Luo, E. Stride, M. Edirisinghe, Mapping the influence of solubility and dielectric constant on electrospinning polycaprolactone solutions, Macromolecules 45 (2012) 4669–4680, https://doi.org/10.1021/ma300656u.
[56] W. Wang, A.H. Barber, Measurement of size-dependent glass transition temperature in electrospun polymer fibers using AFM nanomechanical testing, J. Polym. Sci. Part B Polym. Phys. 50 (2012) 546–551, https://doi.org/10.1002/polb.23030.
[57] S. Curgul, K.J. Van Vliet, G.C. Rutledge, Molecular dynamics simulation of size-dependent structural and thermal properties of polymer nanofibers, Macromolecules 40 (2007) 8483–8489, https://doi.org/10.1021/ma0714666.
[58] S. Budavari (Ed.), The Merck Index An Encyclopedia Of Chemicals, Drugs, And Biologicals, Merck & Co., Inc, 1996.
[59] B. Elvers (Ed.), Ullmann's Food and Feed, Wiley-VCH, 2017.
[60] R. Carmel, How I treat cobalamin (vitamin B12) deficiency, Blood 112 (2008) 2214–2221, https://doi.org/10.1182/blood-2008-03-040253.